



# HHS Public Access

Author manuscript

*Cancer Immunol Res.* Author manuscript; available in PMC 2019 December 01.

Published in final edited form as:

*Cancer Immunol Res.* 2019 June ; 7(6): 939–951. doi:10.1158/2326-6066.CIR-18-0733.

## CD28 homolog is a strong activator of natural killer cells for lysis of B7H7<sup>+</sup> tumor cells

Xiaoxuan Zhuang<sup>1</sup> and Eric O Long<sup>1,\*</sup>

<sup>1</sup>Laboratory of Immunogenetics, National Institute of Allergy and Infectious Diseases, National Institutes of Health, Rockville, United States.

### Abstract

The CD28–B7 family of receptor–ligand pairs regulates lymphocyte responses through costimulation and coinhibition. It includes checkpoint inhibitors, such as PD-1, which limit antitumor and antiviral T-cell responses. CD28 homolog (CD28H) and B7H7 have been identified as a receptor–ligand pair in this family, which has costimulatory activity in T cells. Here we show that CD28H is expressed in primary natural killer (NK) cells and that it is a strong activator of NK cells through selective synergy with receptors NKp46 and 2B4 to induce degranulation, lysis of target cells, and production of proinflammatory cytokines. Expression of B7H7 on target cells enhanced both natural and antibody-dependent cellular cytotoxicity of NK cells. Mutation of tyrosine 192 on the CD28H cytoplasmic tail abolished NK-cell activation through CD28H. As B7H7 is broadly expressed in tumor tissues, we engineered a CD28H chimeric antigen receptor (CD28H-CAR) consisting of full-length CD28H fused to the cytoplasmic domain of T cell receptor  $\zeta$  chain. Remarkably, expression of CD28H-CAR in NK cells triggered lysis of B7H7<sup>+</sup> HLA-E<sup>+</sup> tumor cells by overriding inhibition by the HLA-E receptor NKG2A. The cytoplasmic domains of CD28H and of the  $\zeta$  chain were both required for this activity. Thus, CD28H is a powerful activation receptor of NK cells that broadens their antitumor activity and holds promise as a component of NK-based CARs for cancer immunotherapy.

### Keywords

NK cell; inhibitory receptor; cytotoxicity; chimeric antigen receptor; immunotherapy

### Introduction

NK cells are central components of the innate immune system due to their contribution to defense against pathogens and immune surveillance of tumors (1). Clinical data have shown that higher infiltration of NK cells into tumors correlates with better therapeutic outcomes (2). Tumor tissues often express ligands for NK-cell activation receptors, such as NKG2D ligands MICA/B and ULBP, and DNAM-1 ligand CD155. NK cells can kill transplanted

\*Correspondence: Eric O. Long, 5625 Fishers Lane, 4S12A, MSC 9418, Rockville, Maryland 20892-9418, Phone number: 301-761-5026, eLong@nih.gov.

Competing interests

The authors declare that no competing interests exist.

tumors and spontaneous tumors depending on engagement of NK cell activating receptors by the ligands on tumors cells (1,3). Activation of NK cells requires synergy of specific pairs of coactivation receptors (4,5). Previous studies have shown that only Fc receptor Fc $\gamma$ RIIIa (CD16) is sufficient for activation of cytotoxicity by resting NK cells. NK-cell activation by other receptors requires coengagement of selective receptor pairs, such as 2B4 in synergy with NKG2D or NKp46 (4). The synergistic requirement for activation provides a balance between effective immune surveillance and the risk of autoimmune pathology. Besides direct killing of target cells, NK cells also contribute to early immune responses by secreting cytokines and chemokines (5). Unlike T and B cells, which use a large repertoire of receptors to achieve antigen specificity, NK-cell activity is regulated by a limited number of germline-encoded receptors. NK-cell activation is controlled by MHC class I-specific inhibitory receptors, such as killer cell immunoglobulin-like receptors (KIR) and NKG2A(5). The specificity and breadth of NK-cell reactivity is determined by a repertoire of activating receptors, some of which may not have been discovered yet.

Here we identify CD28 homolog (CD28H, encoded by *TMIGD2*) as an activation receptor in human NK cells. CD28H belongs to the CD28 family of immune receptors, which includes regulators of the immune system, such as checkpoint inhibitors PD-1 and CTLA-4 (6). CD28H was initially described as a molecule involved in cell-cell interaction, cell migration, and angiogenesis of epithelial and endothelial cells (7,8). CD28H has a single extracellular immunoglobulin domain followed by a transmembrane domain and a 110 amino acid-long cytoplasmic region (7,8). CD28H is a costimulatory receptor in naïve T cells (9). The ligand of CD28H is B7 homolog 7 (B7H7 (10), also known as B7-H5, encoded by *HHLA2*), which costimulates T-cell growth and cytokine production (9). Besides expression on antigen presenting cells (APC) after stimulation, B7H7 is also broadly expressed in tumor tissues (9,11–16). CD28H<sup>+</sup> naïve and memory T cells show diminished effector function and increased naïve features (17). CD28H expression has been described on NK cells, innate lymphoid cells (ILCs), and plasmacytoid dendritic cells (pDC) in human peripheral blood (9,17).

The function of CD28H in NK cells is unknown. In this study, we found that CD28H selectively synergized with other activation receptors, such as NKp46 and 2B4, to stimulate NK-cell degranulation and cytotoxicity. CD28H also enhanced NK-cell activation through CD16 for antibody-dependent cellular cytotoxicity (ADCC). We found that a tyrosine at position 192 (Tyr192) of CD28H was essential for phosphorylation and function of the receptor. Furthermore, a CD28H chimeric antigen receptor (CD28H-CAR) was made by fusing full-length CD28H to the intracellular domain of T cell receptor (TCR)  $\zeta$  chain. Expression of CD28H-CAR on NK cells could overcome NKG2A-mediated inhibition due to HLA-E expression on target cells. *In vitro* antitumor activity of the CD28H-CAR showed promising therapeutic potential.

## Materials and Methods

### Plasmids

A plasmid containing B7H7 cDNA was obtained from Harvard PlasmID Database (#HsCD00044662). B7H7 cDNA was amplified and cloned into the EcoRI and NotI cloning

sites of pAc5.1/V5-His A vector (Thermo Fisher Scientific) for expression in *Drosophila* S2 cells, and the EcoRI and NotI cloning sites of pCDH-EF1-T2A-Puro vector (System Biosciences) for expression in human cell lines. The cDNA of CD28H was obtained from Harvard PlasmID Database (#HsCD00416184) in the vector pLX304. CD28H cDNA was amplified and cloned into the EcoRI and NotI cloning sites of pCDH-EF1-T2A-Puro lentivirus vector (System Biosciences) for transduction of human cell lines. CD28H mutants and chimeras were generated using the In-Fusion HD cloning kit (Clontech) and verified by sequencing. All of the cDNAs cloned into the PCDH vector were in frame with the 2A-peptide. Expressed proteins could be detected by anti-2A antibody in immunoblots. All plasmid constructions were carried out using the In-Fusion HD cloning kit (Clontech).

## Cells

Human NK cells were isolated from peripheral blood of healthy U.S. donors by negative selection (STEMCELL Technologies). NK cells were resuspended in Iscove's modified Dulbecco's medium (IMDM; Gibco) supplemented with 10% human serum (Valley Biomedical) and used within 4 days. IL2 and PHA activated NK cells were cultured as described previously (18). Briefly, freshly isolated NK cells were cultured with irradiated autologous feeder cells in OpTimizer (Invitrogen) supplemented with 10% purified IL2 (Hemagen), 100 units/ml recombinant IL2 (Roche) and 5 µg/ml phytohemagglutinin (PHA, Sigma), and expanded in the same medium without PHA and feeder cells. CD28H expression was tested after 2 weeks of activation. To obtain NK cells activated by NKp46 and CD2 plus IL2, freshly isolated NK cells were cultured in plates coated with 5 µg/ml CD2 and NKp46 mAbs, in the presence of 100 units/ml recombinant IL2 (Roche). CD28H expression was tested at day 3, day 5, and day 7. NKL cells (obtained from M. J. Robertson, Indiana University Cancer Research Institute, Indianapolis, IN) and KHYG-1 cells were cultured in IMDM Medium (Gibco) supplemented with 10% heat-inactivated fetal calf serum (Gibco), 2 mM L-Glutamine (Gibco), and 100 units/ml recombinant IL-2 (Roche). 721.221 cells (referred to as 221 cells), P815 cells (obtained from American Type Culture Collection, Manassas, VA), Daudi cells (ATCC Manassas, VA) and HDLM-2 cells (19) (obtained from T. Waldmann, NCI, NIH) were cultured in RPMI 1640 medium (Gibco) containing 10% heat-inactivated fetal calf serum (Gibco) and 2 mM L-Glutamine (Gibco). 221 cells transfected with HLA-E (221.AEH), which included the HLA-A signal peptide to achieve proper HLA-E expression (20), were a gift from D. Geraghty (Fred Hutchinson Cancer Research Center, Seattle). Lenti-X 293T cells (Clontech) were cultured in DMEM medium (Gibco) supplemented with 10% heat-inactivated fetal calf serum (Gibco) and 2 mM L-Glutamine (Gibco). Cells were mycoplasma-free, as tested by the NIH Office of Research Services. All cell lines used were maintained in culture for no longer than 2 months after thawing, and were authenticated by morphology, growth characteristics, expression of surface markers, and functional assays.

## Transfection and lentivirus production

For S2 cells transfection, cells were transfected with plasmids for CD48 and B7H7 expression, both together or each one alone, together with a pAc5.1/V5-His A-puro plasmid for selection in 6 µg/ml puromycin at 1/10<sup>th</sup> the amount of the expression plasmids. Resistant cells were cloned, and tested for CD48 and B7H7 expression. For production of

lentivirus, low-passage Lenti-X 293T cells (Clontech) were plated in a T75 flask 1 day before transfection. Cells were transfected with PEI Max (Polyethylenimine). Briefly, plasmids pMD2.G 1.2 µg, psPAX2 2.3 µg, PCDH 4.6 µg and 217 µl serum-free DMEM were mixed in a 15 ml Falcon tube. 65 µl of PEI Max 40K (Polysciences) stock solution (1 mg/ml) were added, and samples were vortexed briefly. After 10 min at room temperature, 8.6 ml DMEM media with 10% FCS were added to the tube. Culture medium for the 293T cells was replaced with the fresh medium containing the transfection reagent mixture. 2 days after transfection, supernatants were collected, passed through a 0.45 µm filter, aliquoted and stored at -80°C. Supernatants for transduction were used either directly or after enrichment with PEG-*it* (System Biosciences) to increase virus titer. For transduction of human cell lines, lentivirus was added to cells together with polybrene to a final concentration of 8 µg/ml, and incubated for 2 days. Cells were centrifuged at 1200 rpm for 10 min, and resuspended in complete medium with pre-titrated concentrations of puromycin. Surface expression of transduced genes on puromycin-resistant cells was verified by flow cytometry.

### Flow cytometry assays

Most flow cytometry assays were performed by incubating cells with premixed fluorophore-conjugated antibodies at 4°C for 30 minutes. Staining for HLA-E was performed by first incubating cells with anti-HLA-E (3D12) or control mouse IgG1 (clone MOPC-21), followed by PE-conjugated polyclonal goat F(ab')<sub>2</sub> anti-mouse IgG Fc (Jackson). NK cells expanded in IL2 were pre-incubated in 10% human serum for 30 minutes on ice to block Fc receptor CD16, prior to staining with antibodies. As resting NK cells were cultured in IMDM containing 10% human serum until use, no further Fc receptor blocking was needed. Cells were washed after staining, and analyzed on a LSR II (BD Biosciences) or LSRFortessa™ X-20 (BD Biosciences). Data were analyzed with FlowJo (FlowJo, LLC).

### Degranulation and cytotoxicity assays

Redirected cytotoxicity assays were performed as described(4). Briefly, P815 cells were incubated with 5 µg/ml of the indicated combinations of mAbs to CD28H (R&D MAB83162), 2B4 (BioLegend 329502), NKp46 (BD 557847), NKG2D (R&D MAB139), CD2 (BD 555323), DNAM-1 (BD Biosciences 559787), CD16 (BD 555404) and CD56 (BD 555513) for 15 minutes at room temperature. Resting NK cells were added at an E:T ratio of 1:2, mixed and gently centrifuged at 300 rpm for 1 minute. After 2 hours at 37°C, cells were stained with Live/Dead-NIR (Thermo Fisher), anti-CD56-Bv421 (BD 562751) and anti-CD107a-PE (BD 555801) and analyzed by flow cytometry. Target cell lysis assays were either performed using the ToxiLight Non-Destructive Cytotoxicity BioAssay Kit (Lonza) following the manufacturer's instruction, or through a flow-based assay. Briefly, NK cells were incubated with PKH67-labeled target cells for 6 hours in IMDM medium with 10% FCS at the indicated E:T ratios. Cells were stained with Live/Dead NIR, and the lysis of target cells were determined by flow cytometry. For CD28H blocking, NK cells were pre-incubated with 10 µg/ml CD28H antibody (R&D Systems) for 15 min before mixing with 221.B7H7 cells. KHYG-1 and NKL cells were rested in complete IMDM medium without IL-2 for 1 day, prior to use in cytotoxicity assays.

## S2 cell mixing and multiple functional assays

Resting NK cells were mixed with transfected S2 cells at an E:T ratio of 1:2. Cells were incubated in IMDM medium with 10% FCS for 2 hours, stained with Live/Dead-NIR, anti-CD56-Bv421 and anti-CD107a-PE, and analyzed by flow cytometry. To stain for intracellular cytokines and chemokines, NK cells and S2 cells were incubated for 1 hour, and in the presence of 3  $\mu$ M GolgiStop (BD Biosciences) for 5 hours. For CD28H blocking, 10  $\mu$ g/ml CD28H antibody (R&D Systems) was pre-incubated with NK cells for 15 min before mixing with S2 cells. Cells were stained with anti-CD107a-PE (BD 555801) and anti-CD56-Bv421 (BD 562751), fixed with 4% paraformaldehyde for 10 min, and permeabilized with the Intracellular Staining Permeabilization Wash Buffer (BioLegend). Cells were stained with anti-IFN- $\gamma$ -APC (BioLegend 506510), anti-TNF- $\alpha$ -BV650 (BioLegend 502937), anti-MIP-1 $\alpha$ -FITC (Invitrogen MA523564) and anti-MIP-1 $\beta$ -PerCP-Cy5.5 (BD 560688). Data were obtained on a LSR II (BD Biosciences) or LSRFortessa™ X-20 (BD Biosciences), and analyzed with FlowJo (FlowJo, LLC).

## ADCC assays

S2 cells were pre-incubated with a rabbit anti-S2 serum diluted 1:10,000 for 15 min at room temperature. Resting NK cells were added at an E:T ratio of 1:2, mixed, and centrifuged at 300 rpm for 1 min. After 2 hours at 37°C in IMDM medium with 10% FCS, cells were stained with Live/Dead-NIR, anti-CD56-Bv421, and anti-CD107a-PE, and analyzed by flow cytometry. For ADCC assays using Rituximab, 221 cells and Daudi cells were pre-incubated with 10  $\mu$ g/ml Rituximab at room temperature for 15 min. Resting NK cells were added at an E:T ratio of 5:1, and incubated for 5 hours. Lysis of target cells was determined using the ToxiLight Non-Destructive Cytotoxicity BioAssay Kit (Lonza) following the manufacturer's instruction.

## Statistical analysis

Statistical analysis was performed with GraphPad PRISM V7. Data were presented as mean  $\pm$  SEM, and compared by two-tailed Mann-Whitney test or Wilcoxon signed-rank test.

## Human donors

Peripheral blood samples from healthy U.S. adults were obtained from the NIH Department of Transfusion Medicine in accordance with the Belmont Report, under an NIH Institutional Review Board-approved protocol (99-CC-0168) with informed written consent.

## Data Sharing Statement

All supporting data are available on request from the corresponding author.

## Results

### CD28H is expressed on primary, resting human NK cells

The majority of freshly isolated, human NK cells expressed CD28H at the cell surface (Fig. 1A). Human NK cells can be divided into CD56<sup>bright</sup> and CD56<sup>dim</sup> NK subsets based on the expression of CD56. The two subsets have distinct phenotypes and properties (21). We

examined CD28H expression in the two NK subsets, and a greater fraction of the CD56<sup>bright</sup> subset expressed CD28H (Fig. 1B). Most of the CD56<sup>bright</sup> NK cells are phenotyped as CD56<sup>bright</sup>CD16<sup>-</sup>KIR<sup>-</sup>NKG2A<sup>+</sup>CD57<sup>-</sup>, and represent a less mature NK cell population (21). Expression of KIR and NKG2A can divide CD56<sup>dim</sup> NK cells into several subsets (Supplementary Fig. S1A) (22). However, no significant difference in CD28H expression was found between CD56<sup>dim</sup> NK cells that were NKG2A<sup>+</sup>KIR<sup>+</sup>, NKG2A<sup>+</sup>KIR<sup>-</sup>, NKG2A<sup>-</sup>KIR<sup>+</sup>, and NKG2A<sup>-</sup>KIR<sup>-</sup> NK (Fig. 1C). CD57 expression can also be used to further separate CD56<sup>dim</sup> NK cells (23). CD57<sup>+</sup> NK cells are mature, terminal differentiated, and have decreased capacity for proliferation (23). A lower proportion of CD57<sup>+</sup> cells expressed CD28H, as compared to the CD56<sup>dim</sup>CD57<sup>-</sup> NK subset (Fig. 1D). *Ex vivo* expanded and activated NK cells are highly cytotoxic and have been used in clinical and basic research for decades (24,25). A well-established strategy for NK cell expansion in culture is the combination of IL2 and PHA in the presence of irradiated autologous PBMC as feeder cells (18,25). CD28H expression on NK cells was lost after 2 weeks in IL2 and PHA (Supplementary Fig. S1B), a result consistent with a quantitative proteomics analysis of immune cells, in which NK cells had been stimulated with IL2 and plate-coated mAbs to CD2 and NKp46 (26). Using the same stimulating conditions, we confirmed the decrease of CD28H expression by immunostaining (Supplementary Fig. S1C). A reduction in the proportion of NK cells that expressed CD28H was observed 3 days after activation, and gradually dropped to ~20% of NK cells after 7 days of activation (Supplementary Fig. S1D). We also tested expression of CD28H on NK cells activated for a shorter time in IL2. CD25 expression was used as a marker for activation (Supplementary Fig. S1E). No significant difference was observed in CD28H expression on CD25<sup>+</sup> and CD25<sup>-</sup> NK cells after activation in IL2 for 24 hours (Supplementary Fig. S1F). The results showed that expression of CD28H decreased only after long-term stimulation and expansion, but not by short-term activation with IL2.

### CD28H synergizes with 2B4 and NKp46 and enhances NK cell activation by CD16

NK-cell degranulation induced by CD28H alone and CD28H co-engaged with other receptors was tested using the redirected cytotoxicity assay (also known as reverse ADCC) (4,27). The FcR<sup>+</sup> mouse cell line P815 was mixed with monoclonal antibodies (mAbs) to CD28H and other receptors and incubated with NK cells. The F(ab')<sub>2</sub> portions of the mAbs bound to their respective NK cell receptors, whereas the Fc fragments bound to FcR on mouse P815 cells. Activation of NK cells and lysis of P815 cells were induced by co-engagement of NK activation receptors (Supplementary Fig. S2A). Strong NK-cell degranulation, determined by staining for CD56 and CD107a, occurred only after co-engagement of CD28H with either 2B4 or NKp46 (Fig. 2A, B), but not with CD2, NKG2D, or DNAM-1 (Fig. 2C–E). CD56<sup>dim</sup> NK cells in peripheral blood are competent in both cytotoxicity and cytokine production, whereas CD56<sup>bright</sup> NK cells are less cytotoxic and have been viewed as cytokine producers (21,28). Therefore, although a slightly greater fraction of CD56<sup>bright</sup> NK cells expressed CD28H (Fig. 1B), NK-cell degranulation was observed only on CD56<sup>dim</sup> NK cells (Fig. 2A), consistent with previous studies (4,29). CD28H also enhanced the NK-cell degranulation induced by CD16 (Fig. 2F). To titrate the response of NK cells to stimulation through CD28H, mAbs to 2B4, NKp46, and CD16 were used at a constant concentration in redirected cytotoxicity assays in the presence of



increasing concentrations of CD28H antibody (Fig. 2G–I). Enhancement of degranulation was observed with as low as 100 ng/ml CD28H antibody, and stimulation reached a plateau at about 5 µg/ml (Fig. 2G–I). Lysis of P815 cells in this redirected cytotoxicity assay was also investigated at different effector to target ratios (Fig. 2J, K). NK cells lysed P815 target cells efficiently upon co-engagement of CD28H with 2B4 and NKp46, and none of the three receptors alone triggered NK cell cytotoxicity (Fig. 2J, K).

Among four commonly used NK cell lines, namely NKL, YTS, KHYG-1, and NK-92, only KHYG-1 expressed CD28H, whereas all four expressed 2B4 and NKp46 (Supplementary Fig. S2B). KHYG-1 cells lysed P815 target cells in the presence of antibodies to CD28H and 2B4, or CD28H and NKp46 (Supplementary Fig. S2C). Therefore, the synergy of CD28H with 2B4 and NKp46 observed with resting NK cells was reproduced with KHYG-1 cells.

### **B7H7 and CD48 coexpression triggers NK-cell degranulation and cytokine production**

To study the synergistic activation of NK cells by CD28H and 2B4 in the context of receptor–ligand interactions, we expressed B7H7 and CD48, either alone or in combination, in *Drosophila* S2 cells (Supplementary Fig. S3A). CD48, which is expressed on most hematopoietic cells, is the ligand of 2B4. NK cells incubated with S2 cells expressing B7H7 (S2.B7H7) or CD48 (S2.CD48) for 2 hours did not degranulate (Fig. 3A). In contrast, S2 cells expressing both B7H7 and CD48 induced NK-cell degranulation (Fig. 3A, B). The results showed that engagement of both CD28H and 2B4 by their respective ligands lead to synergistic activation of NK cells. Coexpression of B7H7 and CD48 on S2 cells induced production of IFN $\gamma$ , TNF $\alpha$ , MIP-1 $\alpha$ , and MIP-1 $\beta$  in primary NK cells (Fig. 3C–F). As observed with NK-cell degranulation, cytokine and chemokine production was triggered only by synergy of CD28H and 2B4, but not by either receptor alone. Moreover, expression of IFN $\gamma$ , TNF- $\alpha$ , MIP-1 $\alpha$ , and MIP-1 $\beta$  was reduced in the presence of a CD28H blocking antibody (Fig. 3C–F), confirming stimulation through CD28H. Although CD48 and B7H7 alone stimulated a small proportion of NK cells to express MIP-1 $\alpha$ , B7H7 and CD48 together induced strong NK cell responses: approximately 70% of NK cells expressed MIP-1 $\alpha$ , and approximately 10% of NK cells had at least 3 different responses (Supplementary Fig. S3B). It is worth noting that degranulating NK cells and IFN $\gamma$ -producing NK cells were only partially overlapping. Moreover, the blocking antibody toward CD28H attenuated all of the NK responses.

### **CD28H enhances CD16-mediated ADCC**

To explore the possible enhancement of NK cell-mediated ADCC by CD28H, assays were performed with a rabbit antiserum to S2 cells (4). S2 cells were precoated with anti-S2 serum, followed by incubation with primary human NK cells. Expression of B7H7 in S2 cells enhanced NK activation in the ADCC assay, whereas expressing both B7H7 and CD48 increased NK degranulation even further (Fig. 4A, B). NK cell–mediated ADCC plays a central role in the mechanism of action of therapeutic antibodies, such as rituximab (anti-CD20) and cetuximab (anti-EGFR) (30). Three MHC class I–deficient cell lines commonly used as targets for NK cells were examined for expression of B7H7 (Supplementary Fig. S4A). B7H7 was expressed by K562 cells, but not Daudi and 221 cells (Supplementary Fig.

S4A). Among these three cell lines, only 221 expressed CD48 (Supplementary Fig. S4A). We transduced 221 and Daudi cells with a lentivirus for expression of B7H7 and obtained bright and uniform expression of B7H7 (Supplementary Fig. S4B). Freshly isolated human NK cells lysed 221 cells expressing B7H7 (221.B7H7) more efficiently than untransfected 221 cells (Supplementary Fig. S4C). The enhanced lysis of 221.B7H7 was blocked by a CD28H specific mAb (Supplementary Fig. S4C). As Daudi and 221 cells are both CD20<sup>+</sup> lymphoblastoid B-cell lines (Fig. 4C), we used rituximab to induce ADCC. Specific lysis of target cells in rituximab-induced ADCC was increased by the expression of B7H7, and the enhancement in killing was specifically blocked by CD28H antibody (Fig. 4D, E). We concluded that the CD28H–B7H7 interaction enhanced natural killing of 221 and Daudi cells by primary NK cells, as well as lysis of 221 and Daudi cells through ADCC.

### **Tyr192 is essential for CD28H-mediated NK-cell activation**

The CD28H cytoplasmic tail includes three tyrosines, which could potentially contribute to transduction of activation signals. We replaced each tyrosine with a phenylalanine, in all possible combinations. CD28H wild-type and each one of the mutants were immunoprecipitated from transfected HEK293T cells after treatment with the tyrosine phosphatase inhibitor pervanadate. Tyrosine phosphorylation was greatly diminished by mutation of either Y192 or Y222 (Fig. 5A). The function of each of the mutants was tested by expressing them in an NK cell line. Exogenous expression of wild-type CD28H in the CD28H<sup>-</sup> 2B4<sup>+</sup> cell line NKL reproduced the synergy of CD28H and 2B4, as shown in the redirected ADCC assay with P815 cells (Fig. 5B). CD28H mutants were expressed in NKL cells to test the contribution of each tyrosine to CD28H-dependent activation of NK cells (Supplementary Fig. S5). Single-site mutation of Y192 (Y192F) abolished synergistic activation by CD28H and 2B4 (Fig. 5C). Lysis of 221.B7H7 cells by NKL cells expressing wild-type CD28H and CD28H mutants was also investigated. Consistent with the redirected cytotoxicity assays, enhancement of killing of 221 cells by B7H7 expression was also lost with mutation Y192F (Fig. 5D), indicating that phosphorylation of Y192 may be essential for NK-cell activation. The Y192F mutation did not alter accumulation of CD28H at the immunological synapse (Fig. 5E, F), suggesting that the accumulation of CD28H and its ability to signal for cytotoxicity were uncoupled. There are multiple stages in the formation of NK cell immunological synapses (31). The accumulation of mutant Y192F at the synapse indicated that signals specifically triggered by Y192 are not required for that stage of synapse formation. In addition to the three tyrosine residues in the cytoplasmic tail, CD28H also contains a proline-rich domain, which may be involved in signal transduction.

### **NK cells with a CD28H-CAR kill B7H7<sup>+</sup> tumor cells by overriding inhibition by NKG2A**

Expression of the CD28H ligand B7H7 is limited to activated myeloid cells (9,11) and tumor cells (16). We have detected marginal expression of B7H7 on monocytes and DCs activated by LPS or poly (I:C) (Supplementary Fig. S6A and S6B). The broader expression of B7H7 in tumor tissues motivated us to explore the possibility of utilizing the CD28H-B7H7 interaction to target tumors in cancer immunotherapies. We constructed two CD28H CARs by fusing full-length or cytoplasmic domain-truncated ( CD) CD28H with the signal transduction domain of the TCR  $\zeta$  chain (Fig. 6A and Supplementary Fig. S7A and S7B). Expression of the CD28H-CARs in NKL cells (Fig. 6A) did not significantly alter the



cytotoxic activity toward untransfected 221 cells (Fig. 6B), and enhanced killing of 221.B7H7 cells (Fig. 6C). The nonclassical MHC-I antigen HLA-E binds inhibitory receptor NKG2A on NK cells and suppresses NK-cell activation (5). To test whether CD28H or CD28H-CARs were capable of overcoming NKG2A-mediated inhibition, 221.AEH cells, which express HLA-E at the cell surface (20), were transfected with B7H7 (Fig. 6D). NK cells express NKG2A (Fig. 6E). Cytotoxicity of NKL.CD28H and NKL.CD28H-CAR cells toward 221.AEH cells was low, presumably due to inhibition by NKG2A (Fig. 6F). Remarkably, NKL.CD28H-TCR $\zeta$  cells killed 221.AEH.B7H7 cells, indicating that NKG2A-mediated inhibition was overcome by the CD28H–B7H7 interaction (Fig. 6G). Expression of wild-type CD28H alone or CD28H–CD-TCR $\zeta$  chimeric receptor in NKL did not overcome NKG2A inhibition, indicating the essential costimulatory function of CD28H in the CD28H-TCR $\zeta$  chimera (Fig. 6G). We used the B7H7<sup>+</sup> Hodgkin's lymphoma cell line HDLM-2 to further test the antitumor activity of CD28H-CARs (Fig. 6H). HDLM-2 cells, which express HLA-E (Fig. 6H), were lysed by the CD28H<sup>+</sup>NKG2A<sup>+</sup> KHYG-1 NK cell line only after blocking the NKG2A–HLA-E interaction with a mAb to NKG2A (Fig. 6I). However, NKL cells expressing the CAR with full-length CD28H achieved efficient killing of the B7H7<sup>+</sup> HLA-E<sup>+</sup> HDLM-2 tumor cells (Fig. 6J), showing that CD28H-CARs have promising antitumor activity and therapeutic potential.

## Discussion

We showed that most NK cells in circulating blood express CD28H, a member of the CD28 receptor family that has been described in T cells (9,32). Co-engagement of CD28H with 2B4 resulted in synergistic activation of freshly isolated NK cells for degranulation, target cell lysis, and expression of cytokines and chemokines. CD28H is an addition to the family of NK cell coactivation receptors and synergizes with 2B4 and NKp46, but not with NKG2D, CD2, or DNAM-1. CD28H expression is turned off during prolonged activation with IL2. Downregulation of CD28H has also been observed in human T cells after antigenic stimulation (9,17). NK cells freshly isolated from peripheral blood, which are commonly referred to as 'resting', are nevertheless fully functional even in the absence of IL2 and IL15. Co-engagement with CD28H also enhanced CD16-mediated NK-cell degranulation and cytotoxicity. Unlike coactivation receptors that require synergy, CD16 signaling in NK cells is sufficient to activate cytotoxicity (4,29). Other activation receptors, such as 2B4, CD2, NKG2D, and DNAM-1 have also been reported to enhance ADCC (4,29,33,34). It will be informative to test if CD28H synergizes with, or enhances signaling by other activating receptors, such as NKp30, NKp44, NKG2C, SLAMF6, SLAMF7, and activating KIRs.

We and others have shown that B7H7 expresses on activated myeloid cells (9,11). Considering the fact that CD48 is broadly expressed on hematopoietic cells, the expression of B7H7 on activated myeloid cells might contribute to the interaction between NK cells and APCs. The involvement of other potential synergies between CD28H and other activation receptors might add another layer of complexity to the regulation of NK–APC interactions and immune homeostasis. In fact, activating receptors such as NKp30 and NKG2D have been reported as regulators of NK–DC interactions (35,36). Besides its costimulatory function, B7H7 can also have a coinhibitory effect on T cells and has been proposed as an

immune checkpoint inhibitor (11,32). In the context of our study, there was no inhibitory effect of B7H7 toward NK cell lines and primary NK cells in the functional assays performed here, including degranulation, target cell lysis, and cytokine expression. However, expression of checkpoint coinhibitory receptors, such as PD-1 and LAG-3, is usually induced or upregulated on NK cells after activation (37,38). It is possible that expression of a coinhibitory receptor for B7H7 is induced on NK cells by activation or other stimulations.

We tested the contribution of B7H7 expressed on cell lines to the activation of NK cells through CD28H. The mutant cell line 221 is sensitive to NK cell cytotoxicity due to the loss of several MHC-I ligands for NK cell inhibitory receptors. Expression of B7H7 on 221 cells rendered them even more sensitive to NK cells. This could be explained by a synergy of CD28H with 2B4, the ligand of which, CD48, is expressed on 221. However, expression of B7H7 on 221 cells that expressed also HLA-E was not sufficient to overcome inhibition by NKG2A expressed on NK cell lines, which is consistent with the dominant inhibitory function of MHC-I specific receptors on NK cells.

The signaling basis of CD28H synergy with 2B4 and NKp46 is unknown. We showed that just one of the three tyrosine residues (tyrosine 192) in the cytoplasmic tail of CD28H is required and sufficient to coactivate NK cell cytotoxicity. Substitution of the other two tyrosines with phenylalanines did not impair CD28H-mediated NK-cell activation. Tyrosine 192 and adjacent amino acids form a sequence motif (YxN) that predicts binding of SH2 domains of the adaptor Grb2 and related proteins. Further investigations may shed light on signals transduced by CD28H.

There has been a growing interest in the use of NK cells in immunotherapy (39–42), prompted in part by the success of hematopoietic stem cell transplantation where NK cells caused minimal graft-versus-host disease while retaining graft-versus-leukemia activity (43). Several antigen-specific CARs, incorporating single-chain antibodies specific for tumor antigens CD19, CD20, and CD138, have been tested in NK cells (44). A CD19scFv-CD28-TCR $\zeta$  CAR expressed in cord blood-derived NK cells induced a cytotoxic response to CD19<sup>+</sup> leukemia cells *in vitro* and in mice, but was sensitive to inhibition by HLA-E on target cells (45). Expression of a third-generation CAR, designed for use in T cells (CD19scFv-CD28-OX40-TCR $\zeta$ ), in primary NK cells by electroporation of RNA resulted in degranulation in response to CD19<sup>+</sup> cells (46). These CAR-expressing NK cells killed target cells expressing HLA-E, but did not overcome KIR-mediated inhibition with HLA-C<sup>+</sup> target cells (46). The development of induced pluripotent stem cell (iPSC)-derived NK cells provides a resource for NK-based cancer immunotherapy (47). CARs designed specifically for activation of NK cells, based on the known synergistic combinations of activation signals, were superior to third-generation T cell CARs (47). Conversely, even the best CARs for NK-cell activation were not optimal in T cells. The best combinations were those that included the transmembrane domain of NKG2D with the two cytoplasmic domains of 2B4 and TCR $\zeta$ . Surprisingly, the reverse orientation of the NKG2D transmembrane domain across the lipid bilayer (NKG2D is a type II transmembrane protein with the N-terminal region in the cytoplasm) did not prevent signaling for activation. These CARs, directed to an ovarian cancer antigen, showed anticancer activity in the NOD/SCID/ $\gamma_c^{-/-}$  mouse xenogeneic model (47).

An alternative and more natural way to reprogram NK cells is by engineering receptors that are activated by recognition of their ligands on tumor cells. For example, coexpression of a TCR $\zeta$ -NKG2D CAR and DAP10 in human NK cells resulted in strong antitumor activity in mouse tumor models (48,49). Likewise, expression of B7H7 on tumor cells offers an opportunity to develop targeted immunotherapies for elimination of B7H7<sup>+</sup> tumor cells. We tested the possibility of using CD28H itself as a CAR by fusing it to the intracellular domain of TCR $\zeta$ . Expression of the CD28H-TCR $\zeta$  CAR in NKL cells did not result in greater sensitivity of 221.B7H7 cells, which are already highly sensitive to lysis by NKL cells expressing CD28H. However, the CD28H-TCR $\zeta$  CAR in NKL cells provided complete resistance to inhibition by NKG2A, as shown with 221 cells coexpressing B7H7 and HLA-E. Resistance to inhibition was also observed with a Hodgkin's lymphoma tumor cell, HDLM-2, that naturally expresses both B7H7 and HLA-E. As expected, CD28H<sup>-</sup> NKG2A<sup>+</sup> NKL cells did not kill HDML-2 cells. Remarkably, expression of the CD28H-TCR $\zeta$  CAR in NKL cells resulted in very efficient lysis of HDML-2 cells, whereas neither the CD28H cytoplasmic tail nor the TCR $\zeta$  chain on their own could overcome inhibition. The natural transmembrane domain and cytoplasmic tail of CD28H can now be added to the list of CAR components for use in NK cells.

Solutions proposed to overcome signaling by inhibitory receptors for MHC class I on NK cells include silencing of inhibitory receptors concomitant with CAR expression in NK cells (39,46), and combining CAR-expressing NK cells with blockade of inhibitory receptors KIR and NKG2A with antibodies (41), some of which are already used in the clinic (43). A simpler and less costly approach is to design NK-tailored CARs that overcome inhibition by KIR and NKG2A in the context of tumor cells expressing HLA-C and HLA-E. As an example, our CD28H-TCR $\zeta$  CAR was completely resistant to inhibition by NKG2A during contact with HLA-E<sup>+</sup> tumor cells. In summary, we have shown that CD28H is an activation receptor of NK cells, and we raised the possibility of utilizing CD28H for design of NK-CARs in order to overcome signaling by inhibitory receptors and to target tumors expressing B7H7.

## Supplementary Material

Refer to Web version on PubMed Central for supplementary material.

## Acknowledgments

We thank T. Waldmann (National Cancer Institute, NIH) for HDLM-2 cells, M. J. Robertson, Indiana University Cancer Research Institute, Indianapolis, IN) for NKL cells, D. Geraghty (Fred Hutchinson Cancer Research Center, Seattle, WA) for 221.AEH cells and 3D12 antibody, and S. Rajagopalan (National Institute of Allergy and Infectious Diseases, NIH) for comments on the manuscript. This research was supported by the Division of Intramural Research, National Institute of Allergy and Infectious Diseases, National Institutes of Health.

Financial support: This research was supported by the Division of Intramural Research, National Institute of Allergy and Infectious Diseases, National Institutes of Health.

## References

1. Cerwenka A, Lanier LL. Natural killer cells, viruses and cancer. *Nat Rev Immunol* 2001;1:41–9 [PubMed: 11905813]

2. Larsen SK, Gao Y, Basse PH. NK cells in the tumor microenvironment. *Crit Rev Oncog* 2014;19:91–105 [PubMed: 24941376]
3. Marcus A, Gowen BG, Thompson TW, Iannello A, Ardolino M, Deng W, et al. Recognition of tumors by the innate immune system and natural killer cells. *Adv Immunol* 2014;122:91–128 [PubMed: 24507156]
4. Bryceson YT, March ME, Ljunggren HG, Long EO. Synergy among receptors on resting NK cells for the activation of natural cytotoxicity and cytokine secretion. *Blood* 2006;107:159–66 [PubMed: 16150947]
5. Long EO, Kim HS, Liu D, Peterson ME, Rajagopalan S. Controlling natural killer cell responses: integration of signals for activation and inhibition. *Annu Rev Immunol* 2013;31:227–58 [PubMed: 23516982]
6. Schildberg FA, Klein SR, Freeman GJ, Sharpe AH. Coinhibitory Pathways in the B7-CD28 Ligand-Receptor Family. *Immunity* 2016;44:955–72 [PubMed: 27192563]
7. Rahimi N, Rezaadeh K, Mahoney JE, Hartsough E, Meyer RD. Identification of IGPR-1 as a novel adhesion molecule involved in angiogenesis. *Mol Biol Cell* 2012;23:1646–56 [PubMed: 22419821]
8. Wang YHW, Meyer RD, Bondzie PA, Jiang Y, Rahimi I, Rezaadeh K, et al. IGPR-1 Is Required for Endothelial Cell-Cell Adhesion and Barrier Function. *J Mol Biol* 2016;428:5019–33 [PubMed: 27838321]
9. Zhu Y, Yao S, Iliopoulou BP, Han X, Augustine MM, Xu H, et al. B7-H5 costimulates human T cells via CD28H. *Nat Commun* 2013;4:2043 [PubMed: 23784006]
10. Flajnik MF, Tlapakova T, Criscitiello MF, Krylov V, Ohta Y. Evolution of the B7 family: co-evolution of B7H6 and Nkp30, identification of a new B7 family member, B7H7, and of B7's historical relationship with the MHC. *Immunogenetics* 2012;64:571–90 [PubMed: 22488247]
11. Zhao R, Chinai JM, Buhl S, Scanduzzi L, Ray A, Jeon H, et al. HHLA2 is a member of the B7 family and inhibits human CD4 and CD8 T-cell function. *Proc Natl Acad Sci U S A* 2013;110:9879–84 [PubMed: 23716685]
12. Zhu Z, Dong W. Overexpression of HHLA2, a member of the B7 family, is associated with worse survival in human colorectal carcinoma. *Oncotargets Ther* 2018;11:1563–70 [PubMed: 29593422]
13. Koirala P, Roth ME, Gill J, Chinai JM, Ewart MR, Piperdi S, et al. HHLA2, a member of the B7 family, is expressed in human osteosarcoma and is associated with metastases and worse survival. *Sci Rep* 2016;6:31154 [PubMed: 27531281]
14. Cheng H, Borczuk A, Janakiram M, Ren X, Lin J, Assal A, et al. Wide Expression and Significance of Alternative Immune Checkpoint Molecules, B7x and HHLA2, in PD-L1-Negative Human Lung Cancers. *Clin Cancer Res* 2018;24:1954–64 [PubMed: 29374053]
15. Cheng H, Janakiram M, Borczuk A, Lin J, Qiu W, Liu H, et al. HHLA2, a New Immune Checkpoint Member of the B7 Family, Is Widely Expressed in Human Lung Cancer and Associated with EGFR Mutational Status. *Clin Cancer Res* 2017;23:825–32 [PubMed: 27553831]
16. Janakiram M, Chinai JM, Fineberg S, Fiser A, Montagna C, Medavarapu R, et al. Expression, Clinical Significance, and Receptor Identification of the Newest B7 Family Member HHLA2 Protein. *Clin Cancer Res* 2015;21:2359–66 [PubMed: 25549724]
17. Crespo J, Vatan L, Maj T, Liu R, Kryczek I, Zou W. Phenotype and tissue distribution of CD28H(+) immune cell subsets. *Oncoimmunology* 2017;6:e1362529 [PubMed: 29209568]
18. Liu D, Peterson ME, Long EO. The adaptor protein Crk controls activation and inhibition of natural killer cells. *Immunity* 2012;36:600–11 [PubMed: 22464172]
19. Ju W, Zhang M, Wilson KM, Petrus MN, Bamford RN, Zhang X, et al. Augmented efficacy of brentuximab vedotin combined with ruxolitinib and/or Navitoclax in a murine model of human Hodgkin's lymphoma. *Proc Natl Acad Sci U S A* 2016;113:1624–9 [PubMed: 26811457]
20. Lee N, Llano M, Carretero M, Ishitani A, Navarro F, Lopez-Botet M, et al. HLA-E is a major ligand for the natural killer inhibitory receptor CD94/NKG2A. *Proc Natl Acad Sci U S A* 1998;95:5199–204 [PubMed: 9560253]
21. Cooper MA, Fehniger TA, Caligiuri MA. The biology of human natural killer-cell subsets. *Trends Immunol* 2001;22:633–40 [PubMed: 11698225]

22. Cooley S, Xiao F, Pitt M, Gleason M, McCullar V, Bergemann TL, et al. A subpopulation of human peripheral blood NK cells that lacks inhibitory receptors for self-MHC is developmentally immature. *Blood* 2007;110:578–86 [PubMed: 17392508]
23. Lopez-Verges S, Milush JM, Pandey S, York VA, Arakawa-Hoyt J, Pircher H, et al. CD57 defines a functionally distinct population of mature NK cells in the human CD56dimCD16+ NK-cell subset. *Blood* 2010;116:3865–74 [PubMed: 20733159]
24. Bachanova V, Miller JS. NK cells in therapy of cancer. *Crit Rev Oncog* 2014;19:133–41 [PubMed: 24941379]
25. Granzin M, Wagner J, Kohl U, Cerwenka A, Huppert V, Ullrich E. Shaping of Natural Killer Cell Antitumor Activity by Ex Vivo Cultivation. *Front Immunol* 2017;8:458 [PubMed: 28491060]
26. Rieckmann JC, Geiger R, Hornburg D, Wolf T, Kveler K, Jarrossay D, et al. Social network architecture of human immune cells unveiled by quantitative proteomics. *Nat Immunol* 2017;18:583–93 [PubMed: 28263321]
27. Vitale M, Bottino C, Sivori S, Sanseverino L, Castriconi R, Marcenaro E, et al. NKp44, a novel triggering surface molecule specifically expressed by activated natural killer cells, is involved in non-major histocompatibility complex-restricted tumor cell lysis. *J Exp Med* 1998;187:2065–72 [PubMed: 9625766]
28. Fauriat C, Long EO, Ljunggren HG, Bryceson YT. Regulation of human NK-cell cytokine and chemokine production by target cell recognition. *Blood* 2010;115:2167–76 [PubMed: 19965656]
29. Bryceson YT, Ljunggren HG, Long EO. Minimal requirement for induction of natural cytotoxicity and intersection of activation signals by inhibitory receptors. *Blood* 2009;114:2657–66 [PubMed: 19628705]
30. Scott AM, Wolchok JD, Old LJ. Antibody therapy of cancer. *Nat Rev Cancer* 2012;12:278–87 [PubMed: 22437872]
31. Orange JS. Formation and function of the lytic NK-cell immunological synapse. *Nat Rev Immunol* 2008;8:713–25 [PubMed: 19172692]
32. Janakiram M, Shah UA, Liu W, Zhao A, Schoenberg MP, Zang X. The third group of the B7-CD28 immune checkpoint family: HHLA2, TMIGD2, B7x, and B7-H3. *Immunol Rev* 2017;276:26–39 [PubMed: 28258693]
33. Bryceson YT, March ME, Ljunggren HG, Long EO. Activation, coactivation, and costimulation of resting human natural killer cells. *Immunol Rev* 2006;214:73–91 [PubMed: 17100877]
34. Liu LL, Landskron J, Ask EH, Enqvist M, Sohlberg E, Traherne JA, et al. Critical Role of CD2 Co-stimulation in Adaptive Natural Killer Cell Responses Revealed in NKG2C-Deficient Humans. *Cell Rep* 2016;15:1088–99 [PubMed: 27117418]
35. Walzer T, Dalod M, Robbins SH, Zitvogel L, Vivier E. Natural-killer cells and dendritic cells: “l’union fait la force”. *Blood* 2005;106:2252–8 [PubMed: 15933055]
36. Ferlazzo G, Tsang ML, Moretta L, Melioli G, Steinman RM, Munz C. Human dendritic cells activate resting natural killer (NK) cells and are recognized via the NKp30 receptor by activated NK cells. *J Exp Med* 2002;195:343–51 [PubMed: 11828009]
37. Hsu J, Hodgins JJ, Marathe M, Nicolai CJ, Bourgeois-Daigneault MC, Trevino TN, et al. Contribution of NK cells to immunotherapy mediated by PD-1/PD-L1 blockade. *J Clin Invest* 2018;128:4654–68 [PubMed: 30198904]
38. Baixeras E, Huard B, Miossec C, Jitsukawa S, Martin M, Hercend T, et al. Characterization of the lymphocyte activation gene 3-encoded protein. A new ligand for human leukocyte antigen class II antigens. *J Exp Med* 1992;176:327–37 [PubMed: 1380059]
39. Carlsten M, Childs RW. Genetic Manipulation of NK Cells for Cancer Immunotherapy: Techniques and Clinical Implications. *Front Immunol* 2015;6:266 [PubMed: 26113846]
40. Fang F, Xiao W, Tian Z. NK cell-based immunotherapy for cancer. *Semin Immunol* 2017;31:37–54 [PubMed: 28838796]
41. Daher M, Rezvani K. Next generation natural killer cells for cancer immunotherapy: the promise of genetic engineering. *Curr Opin Immunol* 2018;51:146–53 [PubMed: 29605760]
42. Guillerey C, Huntington ND, Smyth MJ. Targeting natural killer cells in cancer immunotherapy. *Nat Immunol* 2016;17:1025–36 [PubMed: 27540992]

43. Cooley S, Parham P, Miller JS. Strategies to activate NK cells to prevent relapse and induce remission following hematopoietic stem cell transplantation. *Blood* 2018;131:1053–62 [PubMed: 29358179]
44. Mehta RS, Rezvani K. Chimeric Antigen Receptor Expressing Natural Killer Cells for the Immunotherapy of Cancer. *Front Immunol* 2018;9:283 [PubMed: 29497427]
45. Liu E, Tong Y, Dotti G, Shaim H, Savoldo B, Mukherjee M, et al. Cord blood NK cells engineered to express IL-15 and a CD19-targeted CAR show long-term persistence and potent antitumor activity. *Leukemia* 2018;32:520–31 [PubMed: 28725044]
46. Oei VYS, Siernicka M, Graczyk-Jarzynka A, Hoel HJ, Yang W, Palacios D, et al. Intrinsic Functional Potential of NK-Cell Subsets Constrains Retargeting Driven by Chimeric Antigen Receptors. *Cancer Immunol Res* 2018;6:467–80 [PubMed: 29459477]
47. Li Y, Hermanson DL, Moriarity BS, Kaufman DS. Human iPSC-Derived Natural Killer Cells Engineered with Chimeric Antigen Receptors Enhance Anti-tumor Activity. *Cell Stem Cell* 2018;23:181–92 e5 [PubMed: 30082067]
48. Chang YH, Connolly J, Shimasaki N, Mimura K, Kono K, Campana D. A chimeric receptor with NKG2D specificity enhances natural killer cell activation and killing of tumor cells. *Cancer Res* 2013;73:1777–86 [PubMed: 23302231]
49. Weiss T, Weller M, Guckenberger M, Sentman CL, Roth P. NKG2D-Based CAR T Cells and Radiotherapy Exert Synergistic Efficacy in Glioblastoma. *Cancer Res* 2018;78:1031–43 [PubMed: 29222400]



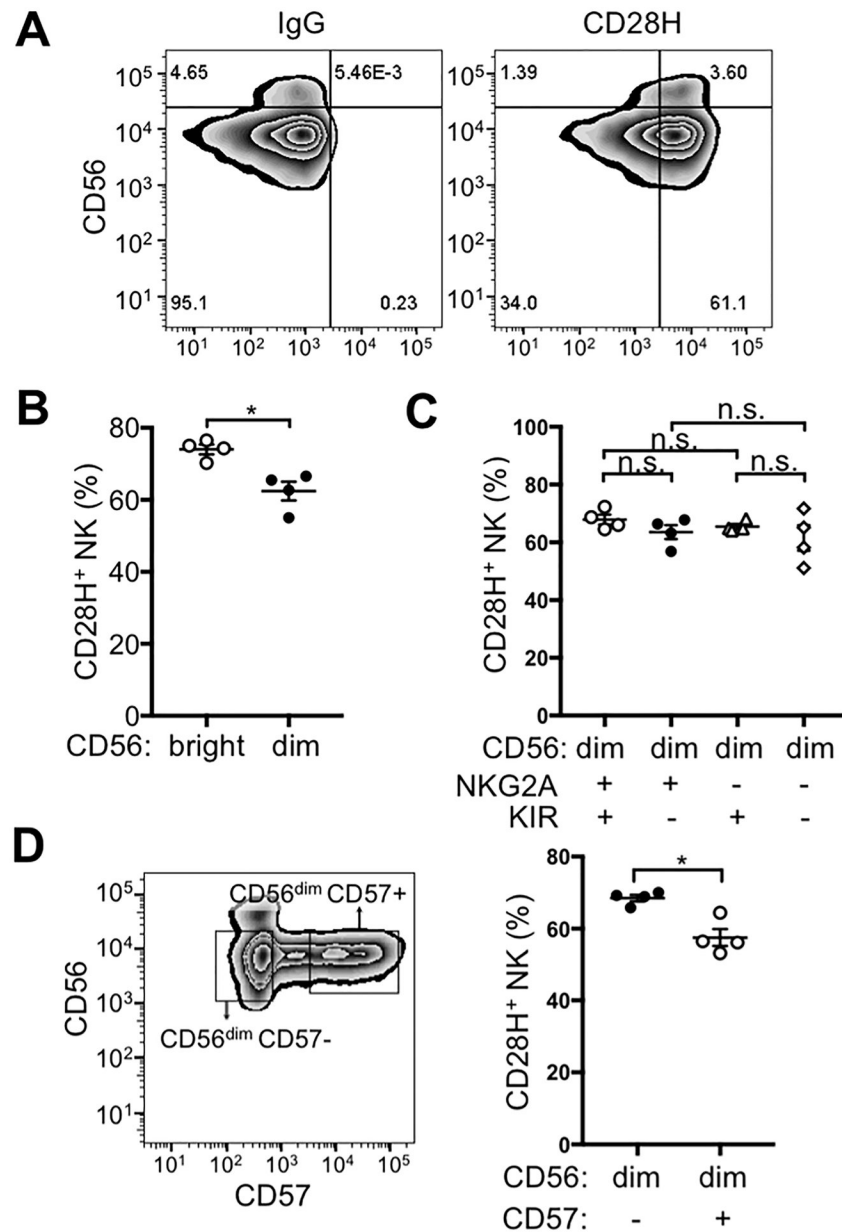


**Figure 1. CD28H expression on human NK cells.**

(A) Freshly isolated NK cells were stained for CD56 and CD28H with fluorophore-conjugated mAbs. An isotype control (IgG) for CD28H is shown in the left panel. (B) Expression of CD28H was compared between CD56<sup>bright</sup> and CD56<sup>dim</sup> NK cells. Each symbol represents an independent donor (n=4). (C) Expression of CD28H in different CD56<sup>dim</sup> subsets defined by KIR and NKG2A expression. Receptors of the KIR family were stained using a cocktail of PE-conjugated antibodies (EB6, GL183 and DX9). Each symbol represents an independent donor (n=4) (D) CD28H expression on CD56<sup>dim</sup>CD57<sup>-</sup> and CD56<sup>dim</sup>CD57<sup>+</sup> NK cells. Each symbol represents an independent donor (n=4). All data are presented as the mean  $\pm$  SEM. \*P<0.05, n.s. not-significant (Mann-Whitney test, two-tailed). All experiments have been repeated at least twice.

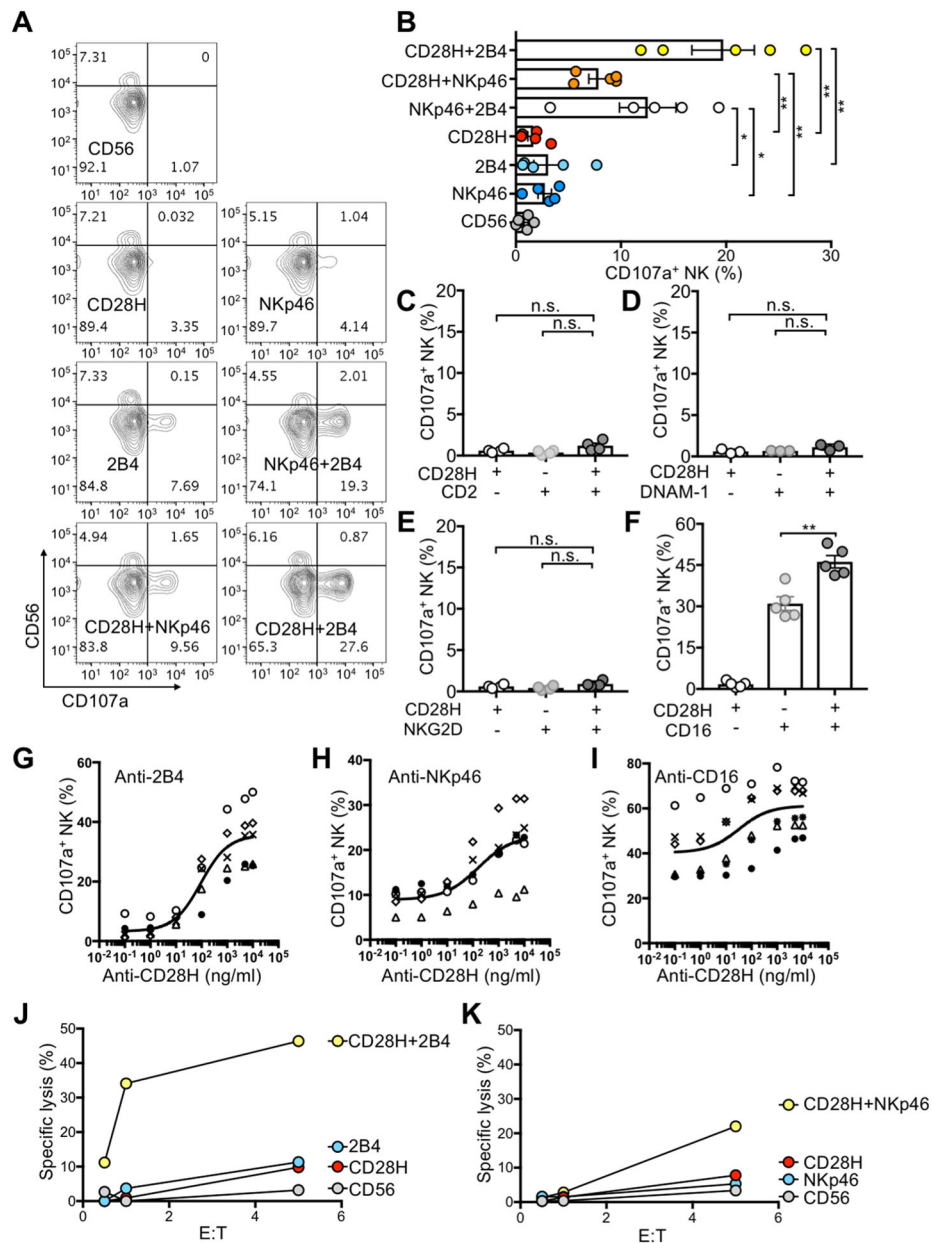


**Figure 2. CD28H synergizes with 2B4 and NKp46 for NK-cell activation and enhances activation through CD16.**

(A) Representative contour plots of NK-cell degranulation induced by CD28H, 2B4, and NKp46, either alone or in combination, in redirected cytotoxicity assays. Freshly isolated NK cells were incubated with P815 cells and 5  $\mu\text{g/ml}$  the indicated mAbs at 37°C for 2 hours. The E to T ratio was 1:2. NK-cell degranulation was determined by staining for CD107a. A mAb to CD56 was a negative control for degranulation, whereas NKp46 and 2B4 co-engagement was a positive control for synergy of NK activating receptors. (B) NK-degranulation as in (A) from several donors. Each symbol represents an independent donor (n=5). (C-F) NK-cell degranulation upon co-engagement of CD28H with CD2 (C), DNAM-1 (D), NKG2D (E) and CD16 (F) in redirected cytotoxicity assays performed as in

(A). Each symbol represents an independent donor, n=4 in (C), n=3 in (D), n=4 in (E), and n=5 in (F). (G-H) NK-cell degranulation as in (A) in redirected cytotoxicity assays. A fixed concentration (5 µg/ml) of mAbs to 2B4 (G), NKp46 (H) and CD16 (I) was used, and CD28H antibody was added at increasing concentrations. Each symbol represents an independent donor, n=5 in (G), n=5 in (H), n=6 in (I). (J, K) NK cells incubated with P815 cells and the indicated mAbs for 6 hours at various E to T ratios. Lysis of P815 cells induced by co-engagement of CD28H with 2B4 (J) or NKp46 (K); each graph represents one of two independent experiments. All data are presented as the mean ± SEM. \*P<0.05, \*\* P<0.01, n.s. not-significant (Mann-Whitney test, two-tailed). All experiments have been repeated at least twice.

Author Manuscript

Author Manuscript

Author Manuscript

Author Manuscript

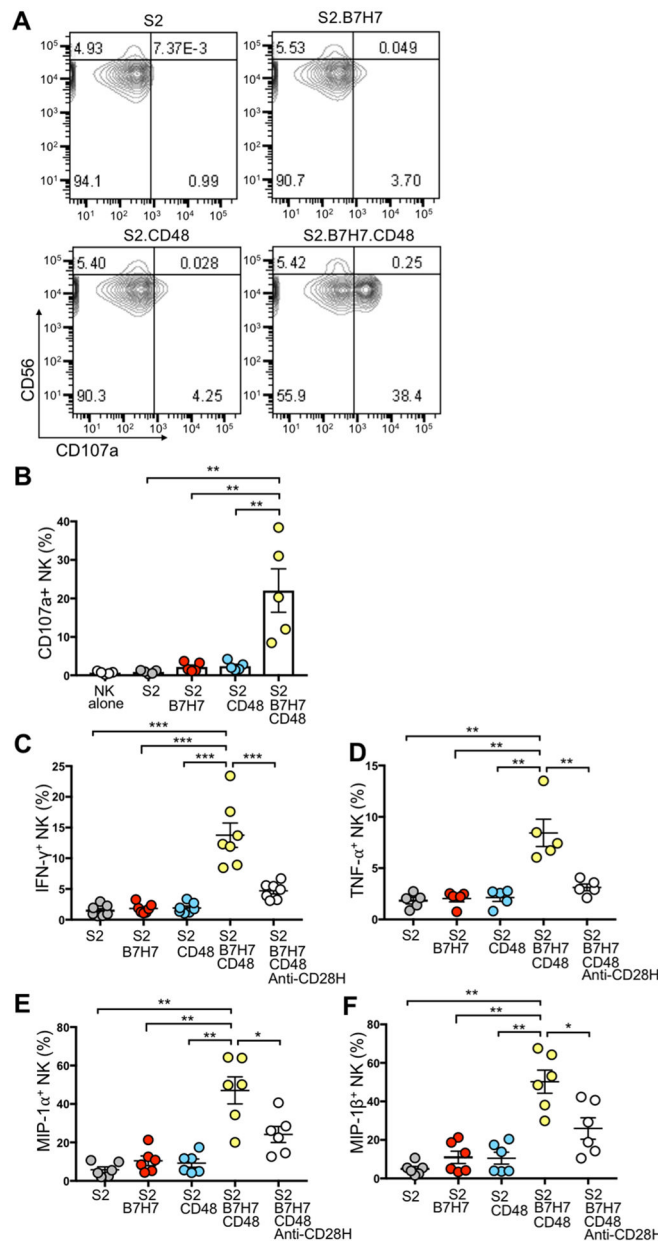


**Figure 3. NK-cell degranulation and cytokine production induced by B7H7 and CD48 on *Drosophila* S2 cells.**

(A) Representative contour plots of NK-cell degranulation induced by S2 cells and S2 cells expressing B7H7, CD48, or both, after incubation for 2 hours at an E:T ratio of 1:2. Degranulation was determined by staining for CD56 and CD107a. (B) NK-cell degranulation as in (A) from several donors. Each symbol represents an independent donor, n=5. (C-F) Cytokine production by NK cells after incubation with the indicated S2 cells at 37°C for 6 hours at an E:T ratio of 1:2. A mAb to CD28H (anti-CD28H) was included at 10 μg/ml to block the B7H7-CD28H interaction. Cells were stained for CD56 and CD107a, fixed and permeabilized, and stained for intracellular cytokines. Expression of IFNγ (C), TNFα (D), MIP-1α (E) and MIP-1β (F) in NK cells from multiple donors. Each symbol

represents an independent donor, n=7 in (C), n=5 in (D), n=6 in (E), and n= 6 in (F). All data are presented as the mean  $\pm$  SEM. \*P<0.05, \*\*P<0.01, \*\*\*P<0.001 (Mann-Whitney test, two-tailed). All experiments have been repeated at least twice.

Author Manuscript

Author Manuscript

Author Manuscript

Author Manuscript

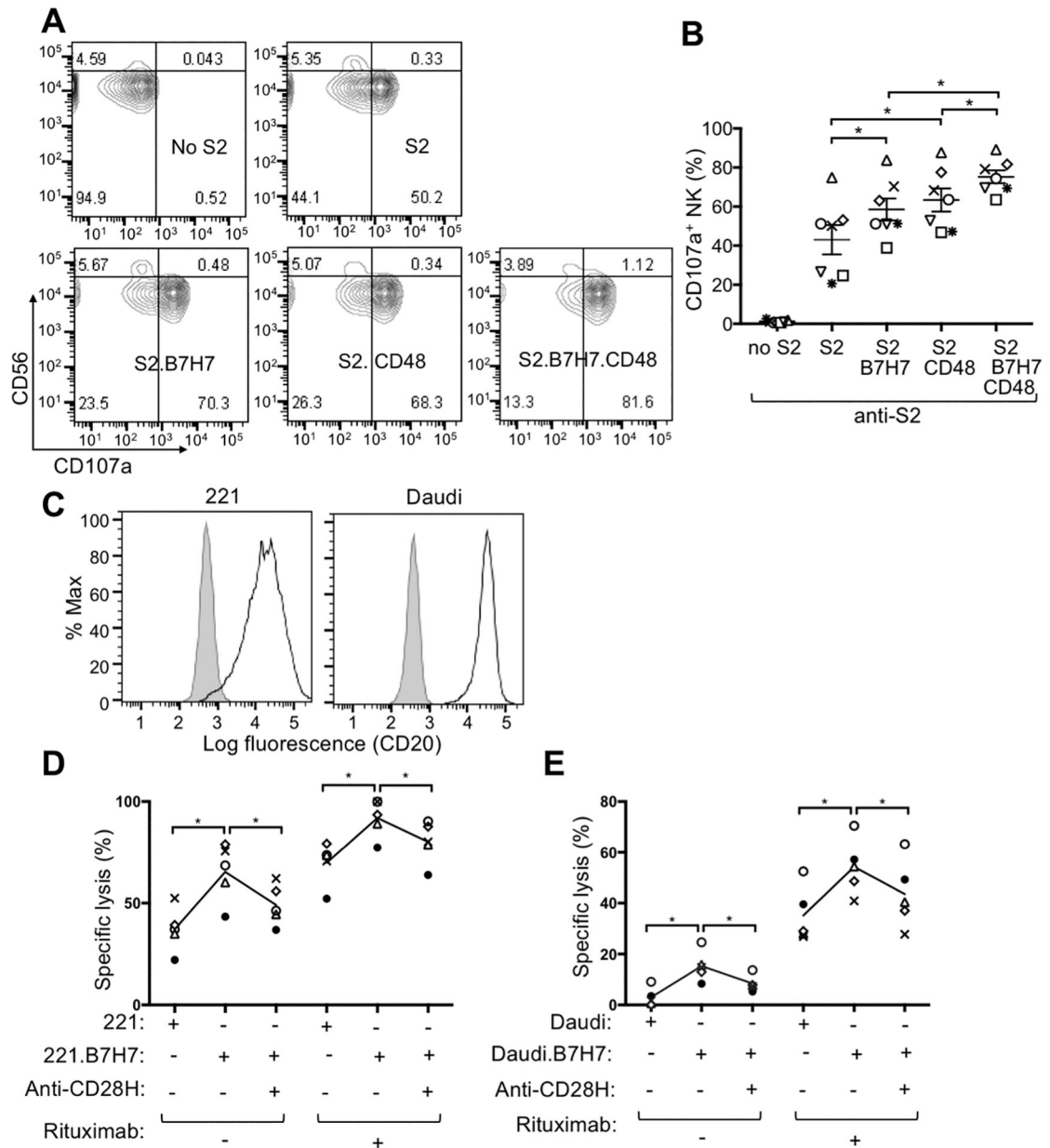


**Figure 4. B7H7 on target cells enhances ADCC by NK cells.**

(A) Representative contour plots of NK-cell degranulation induced by the indicated S2 cells in the presence of anti-S2 serum for 2 hours and measured by staining with fluorophore-conjugated CD56 and CD107a mAbs. (B) Degranulation by NK cells as in (A) from multiple donors. Each symbol represents an independent donor, n=7. (C) Staining for CD20 on 221 and Daudi cells. Shaded histograms indicate staining with isotype control. (D, E) Specific lysis of target cells by NK cells at effector to target cell ratio of 5:1 in the presence of 10 µg/ml Rituximab. Each symbol represents an independent donor, n=5 in both (D) and (E). Target cells were 221 (D) and Daudi (E) cell lines, either untransfected or transfected with B7H7. A mAb to CD28H (anti-CD28H) was included at 10 µg/ml to block the B7H7–



CD28H interaction. All data are presented as the mean  $\pm$  SEM. \*P<0.05 (Wilcoxon signed-rank test, paired, two-tailed). All experiments have been repeated at least twice.

Author Manuscript

Author Manuscript

Author Manuscript

Author Manuscript

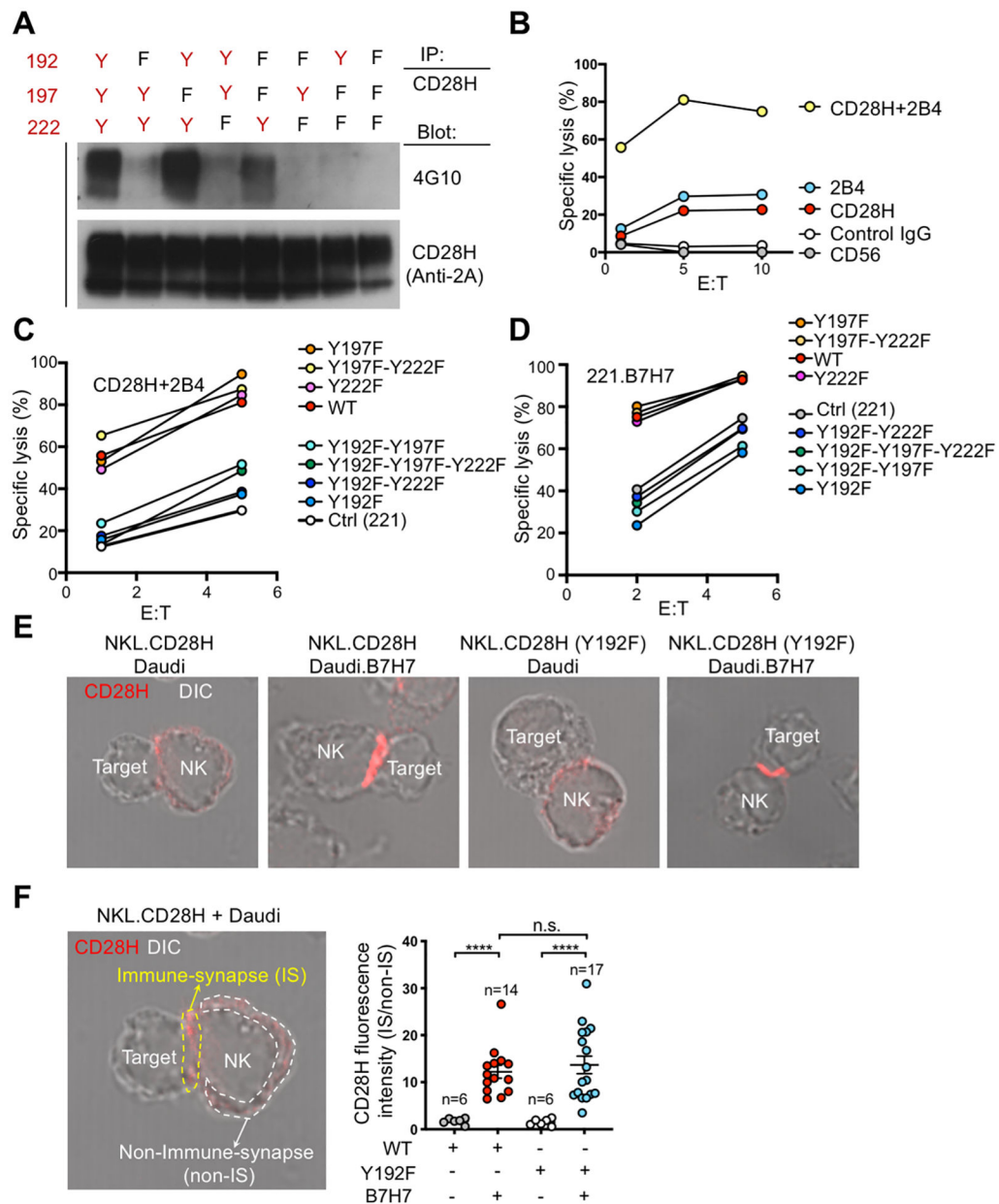


**Figure 5. Tyr192 of CD28H is essential for CD28H-mediated NK-cell activation.**

(A) Tyrosine-phosphorylation of CD28H wild type and the indicated Tyr mutants upon pervanadate treatment. Transfected 293T cells were treated with pervanadate for 10 minutes. Cell lysates were immunoprecipitated with CD28H mAb. Phospho-tyrosine (4G10) and total CD28H (anti-2A) were detected by immunoblots. (B) Lysis of P815 cells by NKL.CD28H cells at various E:T ratios in presence of the indicated mAbs after 6 hours. (C) Lysis of P815 cells by NK cell transfectants in presence of mAbs to 2B4 and CD28H at the indicated E:T ratios. NKL.CD28H-WT with mAb to 2B4 served as negative control (Ctrl). The graph represents one of two independent experiments. (D) Lysis of 221.B7H7 cells by NK cell transfectants at the indicated E:T ratios after 6 hours. Untransfected 221 cells served as negative control. The graph represents one of two independent experiments. (E)

Immunofluorescence staining with CD28H antibody of Daudi or Daudi–B7H7 cells incubated with NKL cells expressing CD28H wild-type or Y192F mutant. (F) Fold change in fluorescence intensity of CD28H at the immunological synapse (IS), as compared to cell surface regions away from the synapse (non-IS), as in (E). Each dot represents a single cell. Sample size (n) is shown in the figure. Data are obtained and combined from two independent experiments and presented as the mean  $\pm$  SEM. \*\*\*\*P<0.0001 (Mann-Whitney test, two-tailed). All experiments have been repeated at least twice.

Author Manuscript

Author Manuscript

Author Manuscript

Author Manuscript

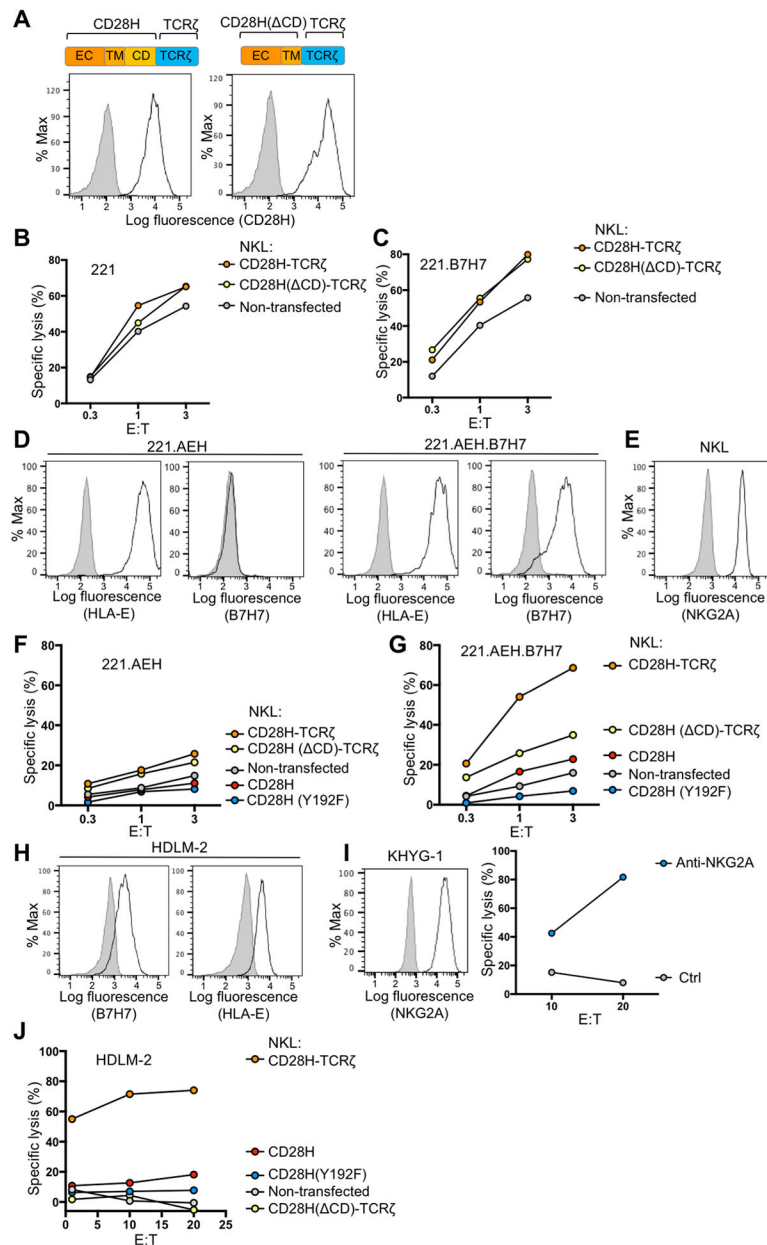


**Figure 6. Lysis of B7H7<sup>+</sup> HLA-E<sup>+</sup> HDLM-2 tumor cells by NKG2A<sup>+</sup> NK cells expressing a CD28H-TCR $\zeta$  chimeric antigen receptor.**

(A) Design and expression of CD28H chimeric antigen receptors in NKL cells. Full-length or cytoplasmic-domain-deleted (CD) CD28H was fused to the cytoplasmic domain of TCR $\zeta$  and transfected into NKL cells. Cells were stained with fluorophore-conjugated CD28H mAb. Shaded histograms represent staining of untransfected NKL cells. (B, C) Lysis of 221 cells (B) and 221.B7H7 cells (C) by transfected NKL cells at the indicated E:T ratio after 5 hours. (D) Staining for HLA-E and B7H7 in 221.AEH and 221.AEH.B7H7 cells. Shaded histograms represent staining of untransfected 221 cells. (E) Expression of NKG2A on NKL cells determined by immunostaining. Shaded histograms represent staining with IgG control. (F, G) Lysis of 221.AEH cells (F) and 221.AEH.B7H7 cells (G) by

transfected NKL cells at the indicated E:T ratios after 5 hours. The graph represents one of two independent experiments. (H) Staining of B7H7 and HLA-E on HDLM-2 tumor cells. Shaded histograms represent staining with isotype controls. (I) Expression of NKG2A on KHYG-1 cells determined by immunostaining (left). Lysis of HDLM-2 tumor cells by KHYG-1 cells after 5 hours, in the presence or absence of a blocking antibody to NKG2A. The graph represents one of two independent experiments. (J) Lysis of HHLA-2<sup>+</sup> HLA-E<sup>+</sup> HDLM-2 tumor cells by transfected NKL cells at the indicated E:T ratio after 5 hours. The graph represents one of two independent experiments. All experiments have been repeated at least twice.

Author Manuscript

Author Manuscript

Author Manuscript

Author Manuscript

Key Resources Table

Reagent type	Designation	Source	Identifier	Monoclonal (M) or Polyclonal (P)	Host & Sub-class	Clone name
Antibody	Anti-human TMIGD2/CD28H	R&D Systems	MAB83162	M	Mouse IgG <sub>2b</sub>	953743
Antibody	Anti-human TMIGD2/CD28H AF647	R&D Systems	FAB83162R	M	Mouse IgG <sub>2b</sub>	953743
Antibody	Anti-human 2B4	BioLegend	329502	M	Mouse IgG <sub>1</sub>	C1.7
Antibody	Anti-human NKG2D	R&D Systems	MAB139	M	Mouse IgG <sub>1</sub>	149810
Antibody	Anti-human NKp46	BD Biosciences	557847	M	Mouse IgG <sub>1</sub>	9-E2
Antibody	Anti-human CD2	BD Biosciences	555323	M	Mouse IgG <sub>1</sub>	RPA-2.10
Antibody	Anti-human DNAM-1	BD Biosciences	559787	M	Mouse IgG <sub>1</sub>	DX11
Antibody	Anti-human CD20 hIgG1 chimera (Rituximab)	Genentech		M		
Antibody	Anti-human CD107a PE	BD Biosciences	555801	M	Mouse IgG <sub>1</sub>	H4A3
Antibody	Anti-human CD107a FITC	BD Biosciences	555800	M	Mouse IgG <sub>1</sub>	H4A3
Antibody	Anti-human CD56 BV421	BD Biosciences	562751	M	Mouse IgG <sub>2b</sub>	NCAM16.2
Antibody	Goat anti-mouse F(ab') <sub>2</sub> PE	Jackson ImmunoResearch	115–116-071	P	Goat	
Antibody	Anti-human CD16	BD Biosciences	555404	M	Mouse IgG <sub>1</sub>	3G8
Antibody	Anti-human CD56	BD Biosciences	555513	M	Mouse IgG <sub>1</sub>	B159
Antibody	Anti-human B7H7	R&D Systems	MAB80841	M	Mouse IgG <sub>1</sub>	907812
Antibody	Anti-human B7H7 AF647	R&D Systems	FAB80841R	M	Mouse IgG <sub>1</sub>	907812
Antibody	Anti-human HLA-E (3D12)	Gift from D. Geraghty (Fred Hutchinson Cancer Research Center, Seattle)		M	Mouse IgG <sub>1</sub>	3D12
Antibody	Anti-human NKG2A (Z199)	Beckman Coulter	IM2751	M	Mouse IgG <sub>2b</sub>	Z199
Antibody	Anti-human IFN $\gamma$ APC	BioLegend	506510	M	Mouse IgG <sub>1</sub>	B27
Antibody	Anti-human TNF $\alpha$ BV650	BioLegend	502937	M	Mouse IgG <sub>1</sub>	MAb11
Antibody	Anti-human MIP-1 $\alpha$ FITC	Invitrogen	MA523564	M	Mouse IgG <sub>2b</sub>	93342
Antibody	Anti-human MIP-1 $\beta$ PerCP-Cy5.5	BD Biosciences	560688	M	Mouse IgG <sub>1</sub>	D21–1351
Antibody	Anti-2A peptide	Millipore	ABS31	P	Rabbit	
Antibody	Anti-phosphotyrosine (4G10)	Millipore (Upstate)	05–321	M	Mouse IgG <sub>2b</sub>	4G10
Chemical compound	Near-IR Dead Cell Stain Kit	Thermo Fisher Scientific	L34975			
Chemical compound	PKH67 Green Fluorescent Cell Linker Kit for General Cell Membrane Labeling	SIGMA Aldrich	PKH67GL			
Commercial kit	In-Fusion HD cloning kit	Clontech Laboratories	639648			
Commercial kit	ToxiLight Non-Destructive Cytotoxicity BioAssay Kit	Lonza	LT07–117			
Commercial kit	EasySep Human NK Cell Enrichment Kit	STEMCELL Technologies	19055			